Supplemental Table 1. Primers used for site-directed mutagenesis of human GGT.

Primer	Sequence
N95Q-F	5'-GGGTGGCCTCTTCCTCACCATCTACCAGAGCACCACACG-3'
N95Q-R	5'-CGTGTGGTGCTCTGGTAGATGGTGAGGAAGAGGCCACC -3'
N120Q-F	5'-GCCACCATGTTCCAGAGCTCGGAGCAGTCCC-3'
N120Q-R	5'-GGGACTGCTCCGAGCTCTGGAACATGGTGGC-3'
N230Q-F	5'-CCCAGGCCTTCTACCAGGGCAGCCTCACGGC-3'
N230Q-R	5'-GCCGTGAGGCTGCCCTGGTAGAAGGCCTGGG-3'
N266Q-F	5'-CGAGCACCCGCTGCAGATCAGCCTGGGAG-3'
N266Q-R	5'-CTCCCAGGCTGATCTGCAGCGGGTGCTCG -3'
N297Q-F	5'-CCTCAAAGGGTACCAGTTCTCCCGGGAGAGCG -3'
N297Q-R	5'-CGCTCTCCCGGGAGAACTGGTACCCTTTGAGG-3'
N344Q-F	5'-GACTGAGGTGGTCCGCCAGATGACCTCCGAG -3'
N344Q-R	5'-CTCGGAGGTCATCTGGCGGACCACCTCAGTC -3'
N511Q-F	5'-CCAGCTTCTGCCCCAGGTCACGACAGTGGAG-3'
N511Q-R	5'-CTCCACTGTCGTGACCTGGGGCAGAAGCTGG-3'
G61L-F	5'-GCACTGCGGGACCTGGGCTCTGCGGTGGATGCAG-3
G61L-R	5'-CTGCATCCACCGCAGAGCCCAGGTCCCGCAGTGC-3'
G62L-F	5'-GCACTGCGGGACGGTCTGTCTGCGGTGGATGCAG-3
G62L-R	5'-CTGCATCCACCGCAGACAGACCGTCCCGCAGTGC-3'
G61L,G62L-R	5'-GGGATGCACTGCGGGACCTGCTGTCTGCGGTGGATGCAGCC-3'
G61L,G62L-F	5'-GGCTGCATCCACCGCAGACAGCAGGTCCCGCAGTGCATCCC-3'
MBW-P1	5'-CACACAGAATTCTCAGCCTCCAAGGAACCT-3'
MBW-P2	5'-CACACAGCGGCCGCGTAGCCGGCAGGCTCCCC-3'

Supplemental Figure 1. Iterative human GGT propeptide homology model building with MODELLER. Five hundred initial models of human GGT (see Methods Section) were built in iteration A followed by three additional iterations (B-D), comprised of 200 models each, which refined loop regions. The DOPE score of each model was used to evaluate the model quality.

Supplemental Figure 2. Additional SDS-PAGE analyses of GGT *N*-glycosylation mutants. (A.) Western analysis against the deglycosylated small subunit of wild-type human GGT and single *N*-glycosylation site mutants to determine relative expression levels. Total cell homogenates (1.5µg) were incubated with 20U of PNGaseF for 18 h at 37˚C and then resolved on a 10% SDS-PAGE followed by immunoblotting against the small subunit of GGT (left panel). Band densities (listed below immunoblot) were defined relative to the wild-type control (1 unit of GGT/1.5µg of protein) as described in the Methods section. An immunoblot against GAPDH is included as a loading control (lower left panel). An immunoblot of an eight-fold (12µg) increase in the sample load from a cell extract expressing the N95Q mutant is included to demonstrate the relative ratio of the expression levels of the mature heteordimer from this allele relative to wild-type GGT (right panel). (B.) Western analysis against the large subunit of wild-type GGT and single *N*-glycosylation mutants expressed in HEK293 cells. Equal expression units of GGT within whole cell lysates from HEK293 cells transfected with either empty vector (lane 1), wild-type GGT (lane 2), or mutant GGT alleles (lanes 3-9) were a resolved by SDS-PAGE and electroblotted onto nitrocellulose. Immunoblotting was conducted using an antibody specific to the large subunit of GGT.

Supplemental Figure 3. Comparative sequence analysis of the *N*-glycosylation sites on human GGT. Amino acid sequence alignment of residues surrounding each of the *N*-glycosylation sites from human (*Homo sapiens*) GGT with the corresponding sequences from pig (*Sus scrofa*), mouse (*Mus musculis*), rat (*Rattus novegicus*), nematode (*Caenorhabiditis elegans*), fission yeast (*Schizosaccharomyces pombe*), and the bacteria *Bacillus subtilis*, *Escherichia coli*, and *Helicobacter pylori* with the ClustalW program (*52*). Shading is used to indicate the occurrence of similar amino acids (identical residues, magenta; conserved substitutions, aquamarine) or putative *N*-glycosylation sites (green shading and arrowheads). The alignment of residues surrounding the universally-conserved catalytic threonine residue at the N-terminus of the small subunit (T381 in human GGT) are also included (red shading) for reference.

Supplemental Figure 4. Homology models of human GGT alleles bearing Loop 3 mutations. (A.-D.) Comparative homology modeling of amino acid substitutions that are predicted to disrupt hydrogen bonding (dashed lines) between the Loop 3 (L3) structure (see Fig. 6) and the common oligosaccharide precursor. (A.) Homology model of the hydrogen bonding interactions predicted to occur between L3 and mannose 6 of the oligosaccharide precursor in the wild-type GGT propeptide. (B.) Homology model of the G61L mutant propeptide, depicting the predicted loss of hydrogen bonding between the oligosaccharide precursor and G62. (C.) Homology model of the G62L mutant propeptide, depicting the predicted loss of hydrogen bonding between the oligosaccharide precursor and L58. (D.) Homology model of the G61L,G62L double mutant that is predicted to disrupt both of the hydrogen bonds between L3 and the oligosaccharide precursor. Leucine was selected as the substituted amino acid at G61 and G62 in order to maximize disruption of L3-glycan interaction while minimizing perturbations to the relative orientation of α-helices 2 and 3. Direct substitutions at L58 that were predicted to disrupt hydrogen

bonding with the *N*-glycan at N95 were also predicted to significantly distort the disulfide-bonded alpha helices and were, thus, avoided.

Supplemental Figure 5. Effects of the Loop 3 mutations on the autocatalytic cleavage of human GGT. (A.) L3 mutations disrupt GGT's enzymatic activity. Total cell lysates from HEK293 cells transfected with wild-type GGT, GGT(N95Q), GGT(G61L), GGT(G62L), or GGT(G61L,G62L) were assayed at 37°C for transpeptidation activity in the presence of 3mM L-GpNA and 40mM glycylglycine, using 2µg of total protein from each extract. Data are the mean +/- SD from triplicate assays. Data are presented as the percent transpeptidation activity relative to wild-type GGT. (B.) L3 mutations inhibit propeptide cleavage. Total cell lysates from HEK293 cells transfected with either wild-type GGT (lane 1), or mutant GGT alleles (lanes 2-5) were resolved by SDS-PAGE and electroblotted onto nitrocellulose, using 4µg of total protein from each extract. Immunoblotting was conducted using an antibody specific to the small subunit of GGT (upper and middle panels). The upper panel depicts the simultaneous detection of both the propeptide and small subunit in the same immunoblot, while the middle panel depicts a prolonged exposure of the region of the blot where the mature small subunit migrated. The faster migration of the propeptide from the GGT(N95Q) mutant is consistent with the loss of glycosylation at N95. An immunoblot against GAPDH is included as a loading control (lower panel). MW, molecular weight markers.

West *et al*., Supplemental Figure 1

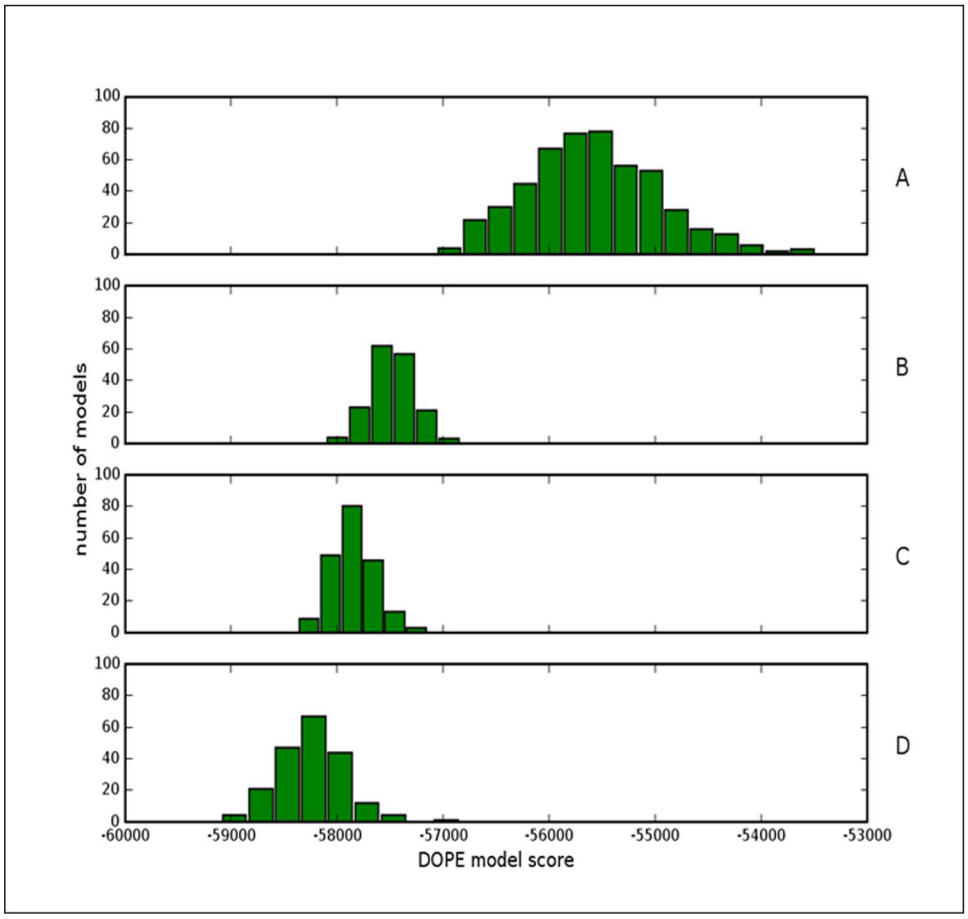

West *et al*., Supplemental Figure 2

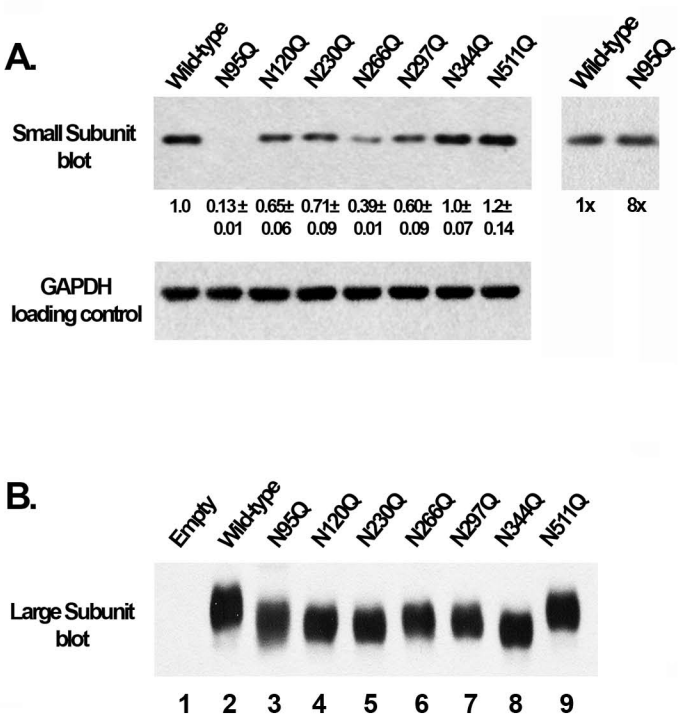

West *et al*., Supplemental Figure 3

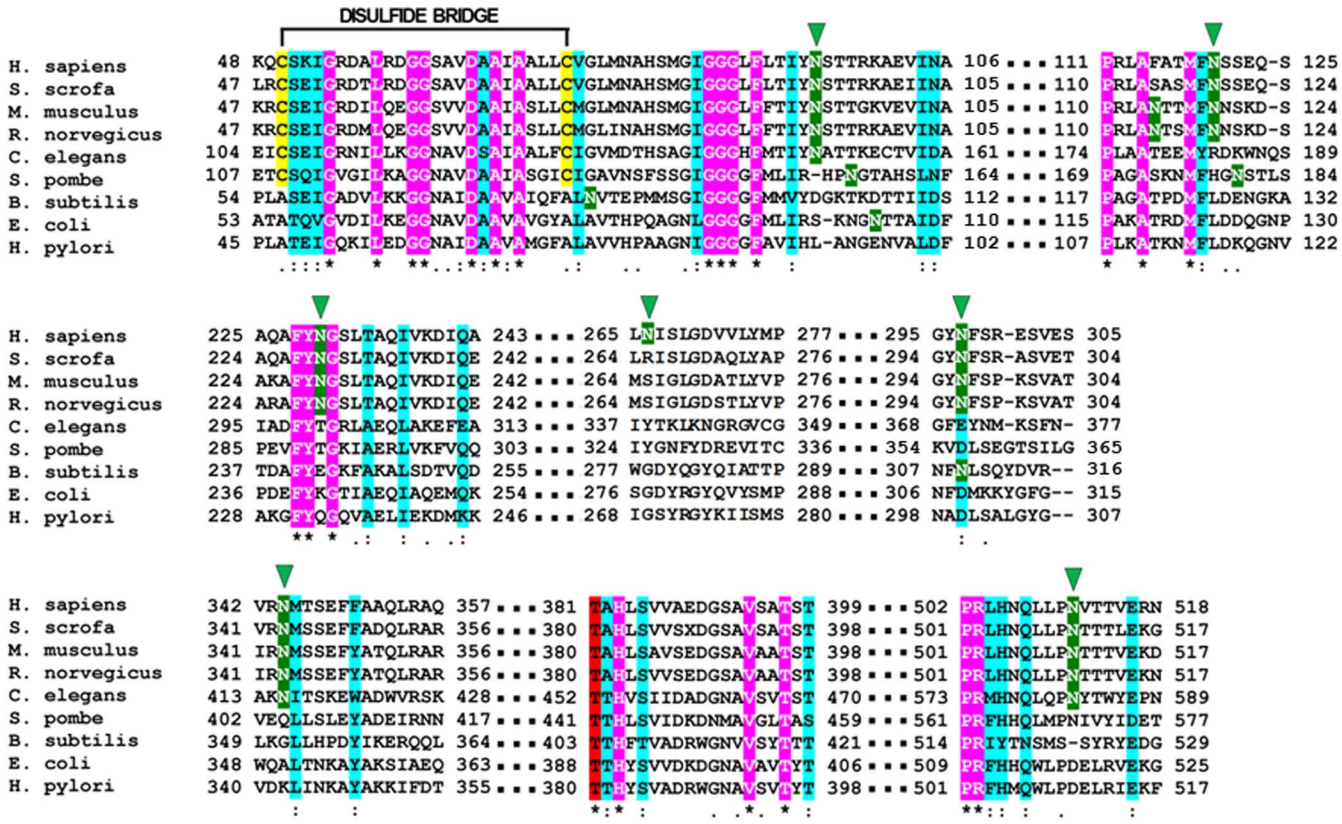

West *et al*., Supplemental Figure 4

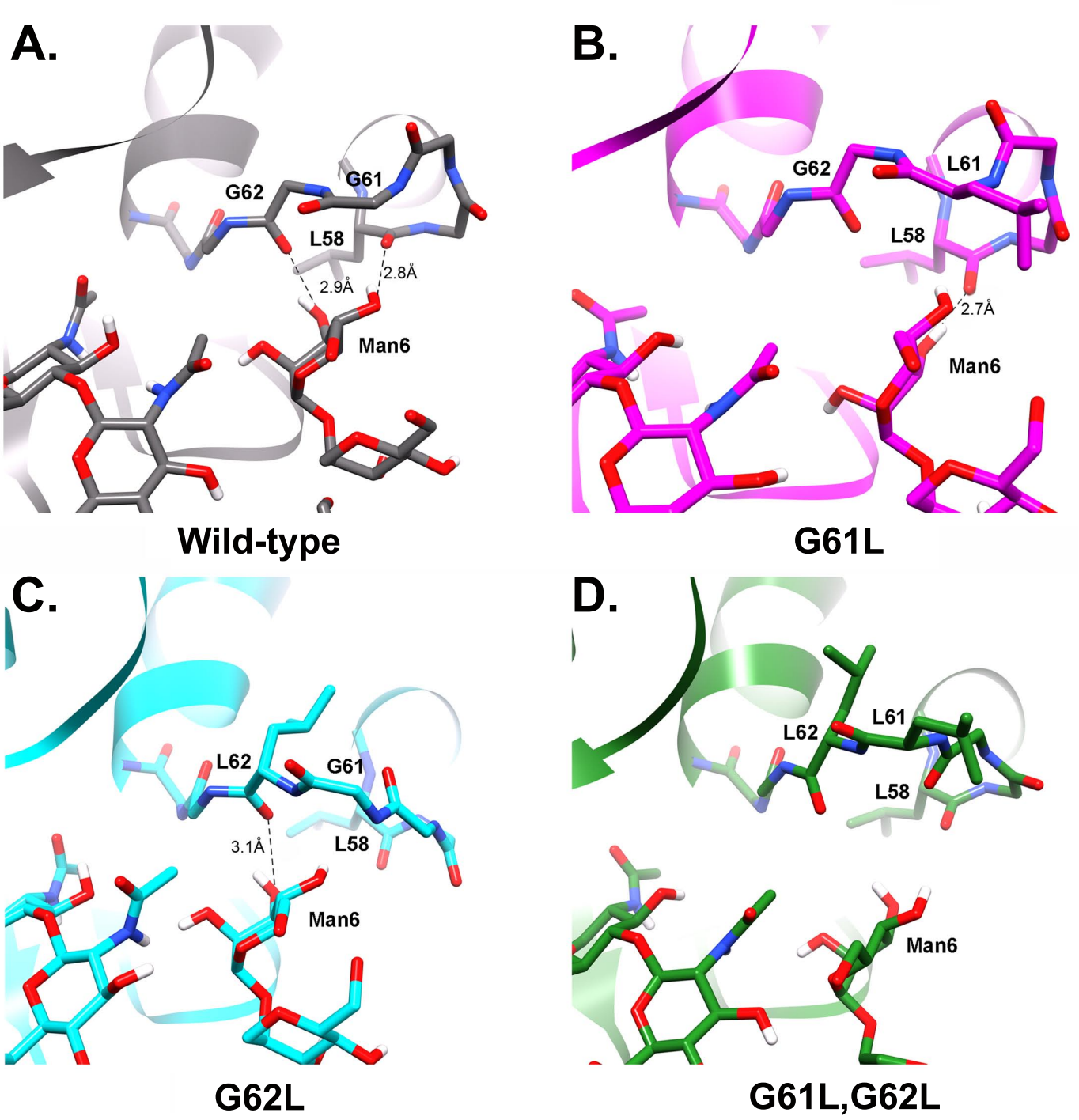

West *et al.*, Supplemental Figure 5